N63-12191
Code 1

NASA

TECHNICAL MEMORANDUM

X-254

PERFORMANCE OF A TURBOJET ENGINE IN COMBINATION WITH AN

EXTERNAL-INTERNAL-COMPRESSION INLET TO MACH 2.88

By David N. Bowditch, Bernhard H. Anderson, and William K. Tabata

Lewis Research Center
Cleveland, Ohio

Declassified July 17, 1962

NATIONAL AERONAUTICS AND SPACE ADMINISTRATION

WASHINGTON   July 1960

NATIONAL AERONAUTICS AND SPACE ADMINISTRATION

TECHNICAL MEMORANDUM X-254

PERFORMANCE OF A TURBOJET ENGINE IN COMBINATION WITH AN

EXTERNAL-INTERNAL-COMPRESSION INLET TO MACH 2.88[*]

By David N. Bowditch, Bernhard H. Anderson, and William K. Tabata

SUMMARY

A turbojet engine was operated in conjunction with an inlet having
external and internal supersonic compression in the Lewis 10- by 10-foot
wind tunnel at several Mach numbers from 2.0 to 2.88. The presence of
the engine had no effect on the steady-state peak inlet performance.
Even though distortions higher than 30 percent of the average total pres-
sure were measured at the compressor face, no engine stall was encountered
during steady-state operation, and there was no significant reduction in
engine performance. However, when the shock regurgitation or unstart
transient pressure drop was large enough, as it was at Mach 2.48 and
above, the engine surged. During engine surge at Mach 2.48, the static
pressure near the engine face reached a value 17 percent higher than the
free-stream total pressure. At Mach 2.68 and 2.88, however, maximum
static pressures during surge were less than the peak pressure due to
buzz.

INTRODUCTION

Turbojet investigations in connected-pipe facilities can simulate
most steady-state conditions encountered in flight. However, transient
conditions imposed on the engine by the inlet require wind-tunnel testing
with an engine-inlet configuration. Similarly, inlet investigations
with a choked plug can obtain the steady-state performance, but the
transient conditions in the inlet are dependent on whether an engine or
plug controls the flow. The steady-state and transient characteristics
of a J34 engine in conjunction with a supersonic inlet were investigated
at Mach numbers to 2.0 and are presented in references 1 to 7. Also, a
nacelle from a current supersonic bomber was tested at Mach numbers of
1.8 and 2.0, and the results are presented in references 8 to 11. How-
ever, none of the inlets previously tested had appreciable internal con-
traction, which is common in most high-performance inlets designed for
Mach numbers of 2.5 and above.

To investigate the engine-inlet problems of shock regurgitation, control of compression surface and terminal shock, and inlet dynamics, the program reported herein was performed. A scaled-up version of the external-internal-contraction inlet described in reference 12 was operated in conjunction with a turbojet engine in the 10- by 10-foot supersonic wind tunnel from Mach 2.0 to 2.88 at angles of attack to 5°. The present report describes the steady-state engine performance and the engine response to terminal-shock regurgitation.

SYMBOLS

M	Mach number
m	air mass flow, slugs/sec
N	engine speed, rpm
N^*	engine design speed, 7460 rpm
P	total pressure, lb/sq ft abs
$\overline{P}_2$	average total pressure at engine inlet
ΔP_2	maximum P_2 minus minimum P_2
p	static pressure, lb/sq ft abs
p_{ce}	transient static pressure at compressor exit
p_{eb}	transient static pressure at engine bypass
p_s	transient static pressure just downstream of spike slot
T	total temperature, °R
W	engine air weight flow, lb/sec
W_f	engine fuel weight flow, lb/sec
α	angle of attack, deg
δ	local P(lb/sq ft) divided by 2116 lb/sq ft
θ	local T(°R) divided by 518.6° R
θ_L	angle between spike axis and straight line joining spike tip and cowl lip, deg

θ_{IGV} angle of inlet guide vanes and first seven state stators from full open position, deg

Subscripts:

0   free stream

2   engine-inlet station

3   turbine-exit station

APPARATUS AND PROCEDURE

Figure 1 shows the external-internal-compression inlet in the 10-by 10-foot tunnel. The supersonic portion of the inlet, which has a cowl-lip diameter of 42 inches, was a scaled-up version of the inlet reported in reference 12. Supersonic compression was obtained through an external oblique shock from the 20° half-angle spike, and from two internal oblique shocks generated by the cowl - each turning the flow about 12°. At the design Mach number, the internal shocks coalesced and impinged on the centerbody at the abruptly turned shoulder. About 2 percent of the captured mass flow was removed through a flush-slot boundary-layer bleed system located immediately forward of the shoulder (fig. 2). Flush slots for boundary-layer control in the vicinity of the terminal shock bled an additional 6 percent of the mass flow at design conditions. The flow furnished by the inlet was matched to the engine requirements by varying the annular choked area between the outside of the bellmouth and the axially translating valve.

The cold-pipe and engine configurations are shown in figure 3. The turbojet engine had a three-stage turbine and a seventeen-stage axial-flow compressor in which the inlet guide vanes and the stators of the first seven stages were variable and remotely controlled. The engine controls regulated engine fuel flow to control engine speed and positioned the exhaust nozzle as a function of throttle position. Since the afterburner flameholder was not installed, the nozzle schedule was modified to compensate for the absence of losses. However, this did not completely correct for the variable flameholder losses; and, as a result, the engine performance deviated from the manufacturers' specifications.

The flow conditions into the engine were measured by two seven-tube rakes mounted at 135° and 328° clockwise from the top, looking at the engine face. These two engine rakes were duplicated, and four similar rakes were added at station 2 in the cold-pipe configuration. The compressor discharge pressure was measured by three rakes of five total tubes each and three wall statics. The exhaust-gas temperature and

4

pressure were measured at the turbine exit by two rakes, each containing seven total tubes and five thermocouples. Engine speed and fuel flow were measured by recording the output of a special engine tachometer and a turbine-type flowmeter. The fuel-meter and engine-tachometer signals were also recorded on an optical oscillograph.

Figure 3 also shows the position where transient static pressures were measured by pressure transducers connected by tubing to static orifices. The estimated natural frequency (in cps) of the tubing and transducer volume, when assumed to be an undamped second-order system, is: just downstream of spike slot (p_s), 300; at engine bypass (p_{eb}), 120; and at compressor exit (p_{ce}), 80. In addition, transient measurements were made with one of the exhaust-gas thermocouples at station 3, whose time constant was 3 seconds.

Inlet distortion and pressure recovery with the engine installed were calculated from the two rakes at the compressor face. Inlet capture mass flow was determined by integration of the conical flow from the 20° spike using the tables of reference 13. The engine mass flow was determined by subtracting the bleed and bypass flows from the captured mass flow. The bleed and bypass flows were estimated from cold-pipe data. The engine performance was corrected by use of the recovery at station 2 and the tunnel total temperature.

The engine-inlet configuration was operated at several Mach numbers from 2.0 to 2.88 at angles of attack from 0° to 5°. The Reynolds numbers per foot varied from 2.3×10^6 to 2.6×10^6 during the investigation. Most steady-state data were taken with the engine operating at the maximum speed, which allowed a bypass airflow of about 5 percent of the capture mass flow at peak recovery. For the transient data presented, the inlet was always unstarted by closing the bypass. No changes were made in the engine control settings and spike or bypass positions for the recording of the transient data presented.

RESULTS AND DISCUSSION

Figures 4 and 5 present most of the engine-inlet conditions tested with the engine configuration. The data taken with the centerbody at the peak recovery or maximum spike-position angle θ_L are shown in figure 4. Total-pressure recovery and compressor-face mass-flow ratio were reduced simultaneously at constant centerbody position and engine speed by increasing the bypass flow. The maximum total-pressure recovery with the engine configuration was within about one count of the best cold-pipe recovery at each Mach number, which shows that the engine does not cause any penalty in steady-state peak total-pressure recovery. At zero angle of attack and a Mach number of 2.88, the distortion increased gradually

from 0.14 at 0.845 recovery to 0.21 at 0.71 recovery. At angle of attack, however, the distortion was much higher and increased much faster as recovery was lowered. This is particularly obvious at 2.5° angle of attack at Mach 2.88, where the distortion increased from 0.24 to 0.37 while the recovery changed only three counts. The distortion at peak recovery and zero angle of attack remained about the same at all Mach numbers. The distortion at 5° angle of attack decreased with reduction in Mach number so that at Mach 2.0 it was comparable with the zero angle-of-attack value.

Engine-inlet conditions over a range of centerbody positions are given in figure 5. At Mach 2.88, the inlet was intentionally set at lower than peak recovery when the spike was extended. However, recovery equal to the cold-pipe value was obtained at least once at each Mach number with the engine configuration, showing that steady-state engine operation causes no reduction in inlet performance. The engine mass-flow ratio is less than the cold-pipe value by the bypass mass-flow ratio. The low internal-contraction or low spike-position-angle (θ_L) performance corresponds to conditions encountered during restarting an inlet at high Mach number. No problem was encountered in operating the engine while the inlet was unstarted, or operating subcritical, at Mach 2.88. Although the recovery was low, the distortion was less than with the inlet started. It was also observed at the time of the test that swallowing the shock during inlet starting did not affect engine performance. Even though the distortion reached 0.27 at spike-extended conditions at Mach 2.88, no engine stall was encountered throughout the steady-state investigation of the entire starting cycle at Mach 2.88.

Some total-pressure contours at the compressor face obtained from cold-pipe data are presented in figure 6. The major cause of distortion was the low-energy air near the hub, which caused a high radial distortion. This type of distortion is probably characteristic of this diffuser, since the centerbody circumference (proportional to local wetted area) at the compressor face is only 28 percent of the shoulder circumference. The maximum circumferential distortion was only about 0.06 at Mach 2.88 and zero angle of attack, and at 5° angle of attack a maximum circumferential distortion of only 0.10, occurring near the cowl, was reached.

Reference 10 states that the engine may have induced a swirl, causing separation at the hub. To investigate this effect, profiles from two sets of identical rakes in the cold-pipe and engine configurations are presented in figure 7. The profiles presented cover a large number of cases; and, while there are small differences, they are not consistent and the majority of the comparisons show almost identical results. Therefore, the engine induced no separation in this configuration.

A summary of the engine performance during the entire test is presented in figures 8(a) to (d). As mentioned in APPARATUS AND PROCEDURE, the performance deviated from the manufacturer's specifications. However, figure 8 indicates that the distortion was not very detrimental to engine performance, even though distortion was higher than 30 percent in some cases. Unpublished data from connected-pipe tests of this engine even show an increase in surge margin as pressure is reduced near the hub. This is not surprising, since the results of connected-pipe tests on other turbojet engines, references 14 and 15, show that distortion affects the engine component and overall performance very little at relatively high speed and that the main effect of distortion is in changing the rotating-stall and surge characteristics, as well as the temperature distribution at the turbine inlet.

Inlet Unstarting

An inlet with internal supersonic compression or contraction has the characteristic of almost instantaneously changing operating conditions from a high recovery condition with internal supersonic compression to operation at relatively low recovery with a normal shock in front of the cowl lip. Shock regurgitation can be caused by either forcing the terminal shock into the converging portion of the inlet where it is unstable (by closing the bypass valve as was done for the data presented herein), or by over-contracting to a point where the inlet throat will not pass all the flow captured by the inlet (by retracting the spike too far). The amount of inlet contraction or internal supersonic compression determines the amplitude of the initial pressure drop at unstarting so that, at Mach 2.0, where the inlet of this report had very little contraction, the unstart pressure drop was of small amplitude. At Mach 2.88, however, where the internal contraction was large, there was a large transient reduction in static pressure as the inlet unstarted. This large transient drop in inlet pressure caused engine surge, which was accompanied in all cases by inlet buzz as will be described more fully.

Static-pressure variations at the rear spike flush slot, the engine bypass, and the compressor exit during two typical shock regurgitations are presented in figure 9. The pressure variations after an inlet unstart at Mach 2.48 are presented in figure 9(a). Pressure pulses from the engine and inlet buzz are both observable in the engine-bypass static-pressure (p_{eb}/P_0) trace and the spike static-pressure (p_s/P_0) trace. The initial static-pressure pulse caused by the engine occurs at 0.05 second and reaches a peak near the engine of p_{eb}/P_0 equal to 1.17 and just downstream of the spike slot of p_s/P_0 equal to 1.02. This and succeeding short pulses are believed to be caused by engine surge, since they immediately follow transient peaks in the static-pressure

ratios across the compressor, as will be shown. Also, it can be seen that the initial increase in the bypass static pressure near the engine occurs before the static pressure near the spike slot begins a steep rise. Two other pulses from the engine are evident at 0.25 and 0.37 second just as the compressor-exit pressure begins to decrease, and again the rise in the bypass static occurs before the corresponding rise in the spike static. In these last two cases, the engine bypass static lead is extremely short. The inlet buzz starts with the pressure rise at 0.11 second and has a period of 0.18 second for the first cycle and about 0.14 second for the second cycle.

Figure 9(b) presents the same pressure variations after an inlet unstarting at optimum inlet contraction and Mach 2.88. As can be seen by the initial pressure drops in p_{eb}/P_0 and p_s/P_0 to 0.374 and 0.243, respectively, the amplitude of the pressure drop due to unstarting was much larger than at Mach 2.48. A combination of this increased pressure drop and the much shorter recovery portion of the buzz cycle between 0.07 and 0.125 second limited the maximum p_{ce}/P_0 to only 3.42. The short engine-surge pulses coincide with the decrease in compressor-exit pressure, but in this case the maximum p_{eb}/P_0 due to surge reaches a value of only 0.530. In fact, the surge amplitude was mild enough in this case that the spike static-pressure trace shows very little response coinciding with the pressure increases due to surge at the engine bypass.

Engine-bypass and compressor-exit static pressures and their ratio, along with the engine speed and exhaust-gas temperature, are presented for 1.5 seconds in figure 10(a) for the transient already described in figure 9(a). Because the engine-bypass static is not at the engine face, the compressor static-pressure ratio is not accurate; but it certainly indicates trends. By comparison of the time history of the engine-bypass static pressure and the compressor static-pressure ratio, it is evident that the peaks in compressor pressure ratio are always followed by the short pulses in the engine-bypass static pressure or the beginning of an inlet buzz cycle. Also, after the peak static pressure during a buzz cycle, the initial short pulse coincides with the start of the sharp decrease in compressor-exit static pressure, showing that these pulses are due to engine surge. From the compressor pressure ratio it can be seen that the engine surges two or more times during each buzz cycle; this causes the speed to decrease and the exhaust-gas temperature to steadily increase. The engine speed decrease reduces the engine airflow, forcing the inlet farther into the buzz region as indicated by the increasing buzz frequency with time. The irregularity in the peak compressor static-pressure ratio reached before surge indicates changes in the engine surge limit. These changes are probably due to changing engine conditions, inlet flow distortion, and variation in the rate of inlet pressure change, which was shown to affect the surge limits in reference 16.

Figure 10(a) is for an engine-inlet guide-vane angle of 3.5° from full open. By closing the inlet guide vanes to 5.1° from full open, thus increasing compressor stall margin, the shock loss transient presented in figure 10(b) was obtained. Even though the peak compressor static-pressure ratio was higher in this case, the engine did not stall, and the inlet was not forced into buzz after unstarting. Although not done in this report, the occurrence of surge could be predicted by an analysis similar to reference 16 if the characteristics of the engine components are known.

During unstarting, the engine-bypass pressure decreases more quickly and reaches a lower value at Mach 2.88 than at Mach 2.48; this causes the compressor pressure ratio to increase in about 0.02 second to a maximum value of better than 14 (fig. 10(c)). The surge pulses that follow are mild and never reach values equal to the peak pressures during buzz. After unstarting, the exhaust-gas temperature increases and the speed continually decreases, forcing the inlet farther into the buzz region.

A summary of pertinent nondimensional engine-bypass static pressure (p_{eb}/P_0) from all the usable transient data obtained during unstarting of the inlet is presented in table I. Each transient is designated by an arbitrary number in the first column for convenience. The next four columns contain the steady free-stream Mach number, engine corrected speed, inlet-guide-vane setting, and inlet spike position just prior to unstarting. The next two columns indicate whether the inlet buzzed or the engine surged after an unstart. The first and second columns under p_{eb}/P_0 present the nondimensional pressure just before the unstarting transient, and the initial minimum p_{eb}/P_0 reached before any surge pulse or buzz. Therefore, during transient 6, which is the same transient presented in figures 9(a) and 10(a), the p_{eb}/P_0 before unstart of 0.745 occurs before zero time in figure 10(a), and the initial minimum p_{eb}/P_0 after unstart of 0.515 occurs at 0.03 second in figure 10(a). During the first second after unstarting, the maximum buzz p_{eb}/P_0 of transient 6 can be seen in figure 10(a) where the upper buzz envelope crosses 0.840 at 1 second. The initial minimum and the maximum p_{eb}/P_0 reached during a short-duration, or surge, pulse correspond to the initial p_{eb}/P_0 of 0.515 and the maximum pressure of 1.17, which occur at 0.03 and 0.05 second, respectively. The initial surge p_{eb}/P_0 and the initial minimum unstart p_{eb}/P_0 do not necessarily coincide as they do in this case. When there is no surge or buzz as in transient 8, which is also presented in figure 10(b), the p_{eb}/P_0 steady non-dimensional pressure of 0.66 occurs after 0.08 second.

Table I indicates that engine surge after an inlet unstart can be related to the corresponding pressure-drop amplitude. No surge or buzz

was encountered where the amplitude of the unstarting pressure drop was small as it was at Mach 2.28 and below, and at Mach 2.88 with the spike at low position angle. The unstarting pressure-drop amplitude at Mach 2.48 must have been a borderline case, as it caused the engine to surge with the inlet guide vanes at 3.3° from full open, but the same pressure transient did not cause surge if the inlet guide vanes were closed to 5.1°. At a Mach number of 2.88 and a spike position of 29.90, where the pressure drop at unstarting is very large, the engine surged after inlet shock regurgitation even when the inlet vanes were closed to 10.2° from full open.

The pressures due to engine surge were measured to be 17 percent higher than free-stream total pressure at Mach 2.48 after an inlet unstart. However, this excess pressure was encountered only at the one condition; and at Mach numbers of 2.68 and 2.88 the maximum pressures due to surge were less than the maximum pressures during the buzz cycle. Since the engine and inlet conditions were very similar before unstarting at all three Mach numbers, the only obvious changes that might have caused the change in peak surge pressure are the increases in amplitude and steepness of the drop in inlet pressure at the higher Mach numbers.

During a total engine running time of 30 hours, 26 minutes the engine-inlet configuration was unstarted into buzz and stall about 25 to 30 times. During the buzz and stall the vibration meters on the engine indicated 8 to 15 mils, but whether this was engine or nacelle vibration is not known. Each time the buzz and stall was encountered, the engine was shut off. The engine operated perfectly at the end of the test, and a visual inspection of the engine without disassembly disclosed no damage in spite of operating in stall and buzz a total of about 3 to 4 minutes.

SUMMARY OF RESULTS

A turbojet engine was operated in conjunction with an external-internal-compression inlet at Mach numbers from 2.0 to 2.88 and angles of attack of 0°, 2.5°, and 5° with the following results:

1. Unstarting of the inlet when the engine and inlet were both operating near peak conditions at Mach numbers of 2.48 and above caused the engine to surge.

2. Engine surge during unstarting caused transient duct static pressures as high as 117 percent of free-stream total pressure.

3. Although radial distortions reached values higher than 30 percent of the average compressor-face total pressure with a circumferential component of 10 percent, no appreciable change in engine performance was observed.

4. Identical rakes in an engine-inlet configuration and a cold-pipe configuration showed that flow separation induced by the engine (as previously reported) was not present in this configuration.

Lewis Research Center
    National Aeronautics and Space Administration
   Cleveland, Ohio, February 24, 1960

REFERENCES

1. Nettles, J. C., and Leissler, L. A.: Investigation of Adjustable Supersonic Inlet in Combination with J34 Engine up to Mach 2.0. NACA RM E54H11, 1954.

2. Beke, Andrew, Englert, Gerald, and Beheim, Milton: Effect of an Adjustable Supersonic Inlet on the Performance up to Mach Number of 2.0 of a J34 Turbojet Engine. NACA RM E55I27, 1956.

3. Beheim, Milton A., and Englert, Gerald W.: Effect of a J34 Turbojet Engine on Supersonic Diffuser Performance. NACA RM E55I21, 1956.

4. Beheim, Milton A., and Evans, Philip J.: Effects of Rocket-Armament Exhaust Gas on the Performance of a Supersonic-Inlet J34-Turbojet-Engine Installation at Mach 2.0. NACA RM E55K22, 1956.

5. Musial, Norman T.: Comparison of Effect of a Turbjet Engine and Three Cold-Flow Configurations on the Stability of a Full-Scale Supersonic Inlet. NACA RM E56K23, 1957.

6. Nettles, J. Cary, and Campbell, Robert C.: Investigation at Supersonic Speeds of the Compressor Stall and Inlet Buzz Characteristics of a J34 - Spike-Inlet Combination. NACA RM E57K19b, 1958.

7. Bowditch, David N., and Wilcox, Fred A.: Dynamic Response of a Supersonic Diffuser to Bypass and Spike Oscillation. NASA TM X-10, 1959.

8. Hearth, Donald P., Anderson, Bernhard H., and Dryer, Murray: Performance Comparison at Mach Numbers 1.8 and 2.0 of Full-Scale and Quarter-Scale Translating-Spike Inlets. NACA RM E57D16, 1957.

9. Hearth, Donald P., and Anderson, Bernhard H.: Use of Constant Diffuser Mach Number as a Control Parameter for Variable-Geometry Inlets at Mach Numbers of 1.8 to 2.0. NACA RM E57G02, 1957.

10. Hearth, D. P., and Musial, N. T.: Investigation of a Supersonic-Inlet Turbojet-Engine Combination at Mach 2.0 and Angles of Attack up to 6°. NACA RM E57D18, 1957.

11. Musial, Norman T., and Bowditch, David: Effects of Free-Stream Reynolds Number, Engine Installation, and Model Scale on Stability Characteristics of a Translating-Spike Inlet at Mach 2.0. NACA RM E57D17, 1957.

12. Obery, Leonard J., and Stitt, Leonard E.: Performance of External-Internal Compression Inlet with Abrupt Internal Turning at Mach Numbers 3.0 to 2.0. NACA RM E57H07a, 1957.

13. Anon.: Tables of Supersonic Flow Around Cones. Rep. No. 1, Dept. Elec. Eng., M.I.T., 1947.

14. Conrad, William, Hanson, Morgan P., and McAulay, John E.: Effects of Inlet-Air-Flow Distortion on Steady-State Altitude Performance of an Axial-Flow Turbojet Engine. NACA RM E55A04, 1955.

15. Huntley, S. C., Sivo, Joseph N., and Walker, Curtis L.: Effect of Circumferential Total-Pressure Gradients Typical of Single-Inlet Duct Installations on Performance of an Axial-Flow Turbojet Engine. NACA RM E54K26a, 1955.

16. Gabriel, David S., Wallner, Lewis E., Lubick, Robert J., and Vasu, George: Some Effects of Inlet Pressure and Temperature Transients on Turbojet Engines. Aero. Eng. Rev., vol. 16, no. 9, Sept. 1957, pp. 54-59.

TABLE I. - SUMMARY OF DATA FROM TRACES OF INLET UNSTARTING

Transient	M_O	$N/N^*\sqrt{\theta}$	θ_{IGV}, deg	θ_L, deg	Buzz?	Surge?	Nondimensional engine-bypass static pressure, p_{eb}/P_O					Comments
							Unstart		Max. buzz or steady	Max. surge		
							Before	Initial min.		Initial	Maximum	
1	2.00	0.941	3.5	26.00	No	No	0.760	0.717	0.717	-----	-----	No overshoot during unstarting
2	2.28	.928	3.5	27.25	→No	→No	.758	.667	.682	-----	-----	Slight overshoot during unstarting
3	2.28	.928	3.5	27.25			.755	.682	.682	-----	-----	No overshoot during unstarting
4	2.48	.942	3.3	28.22	Yes	Yes	.737	.478	.740	.478	1.156	Unstarting causes surge and buzz
5		.896	3.5	28.20			.752	.513	.822	.513	1.153	Unstarting causes surge and buzz
6			3.5				.745	.515	.840	.515	1.173	Unstarting causes surge and buzz
7			5.1		No	No	.745	.540	.665	-----	-----	Closing inlet guide vanes during unstarting prevents surge and buzz
8			5.1				.745	.525	.660	-----	-----	Same as above
9			10.2		→Yes	→Yes	.745	.478	.660	-----	-----	Same as above except IGV's closed more
10	2.68	.882	3.5	28.99	Yes	Yes	.725	.460	.745	.460	.638	Unstarting causes buzz and weak surge
11	2.88	.872	3.3	29.90			.750	.375	.685	.315	.530	Unstarting causes buzz and weak surge
12		.872	7.2	29.90			.750	.312	.775	.291	.553	With IGV's partially closed, unstarting causes buzz and stronger surge
13		.873	10.2	29.90		→	.744	.277	.590	.237	.537	Closing IGV's farther still does not prevent buzz and surge
14		.868	-1.0	28.30	No	No	.581	.523	.523	-----	-----	Reducing pressure drop due to unstarting prevents buzz and surge
15		.868	-1.0	27.76	7 cycles	No	.565	.507	.575	-----	-----	Additional spike extension over above case produces little change
16		.871	3.3	28.54	Yes	Yes	.586	.283	.608	.250	.450	Unstarting from peak recovery at 2.5 causes buzz and surge

E-649
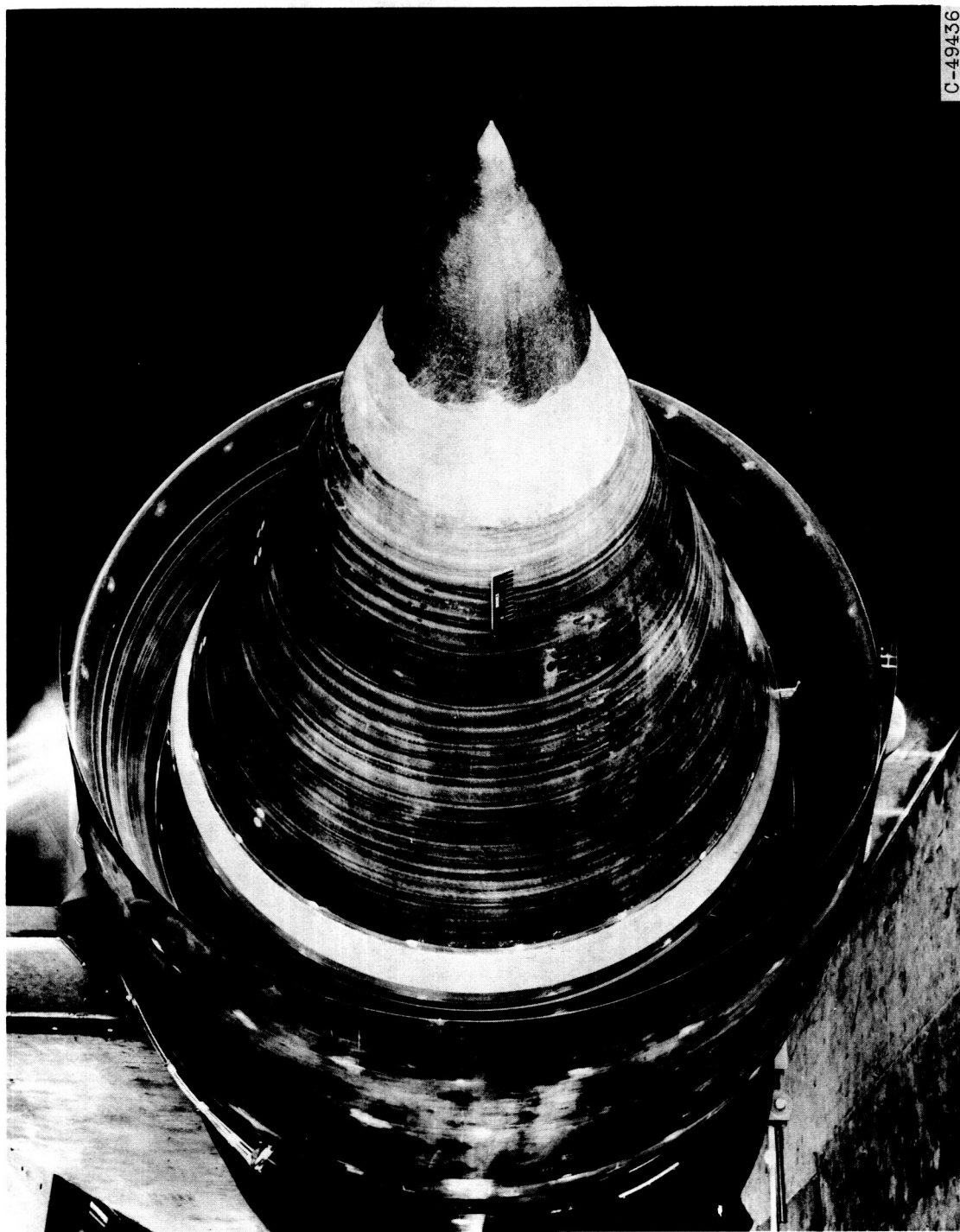
C-49436

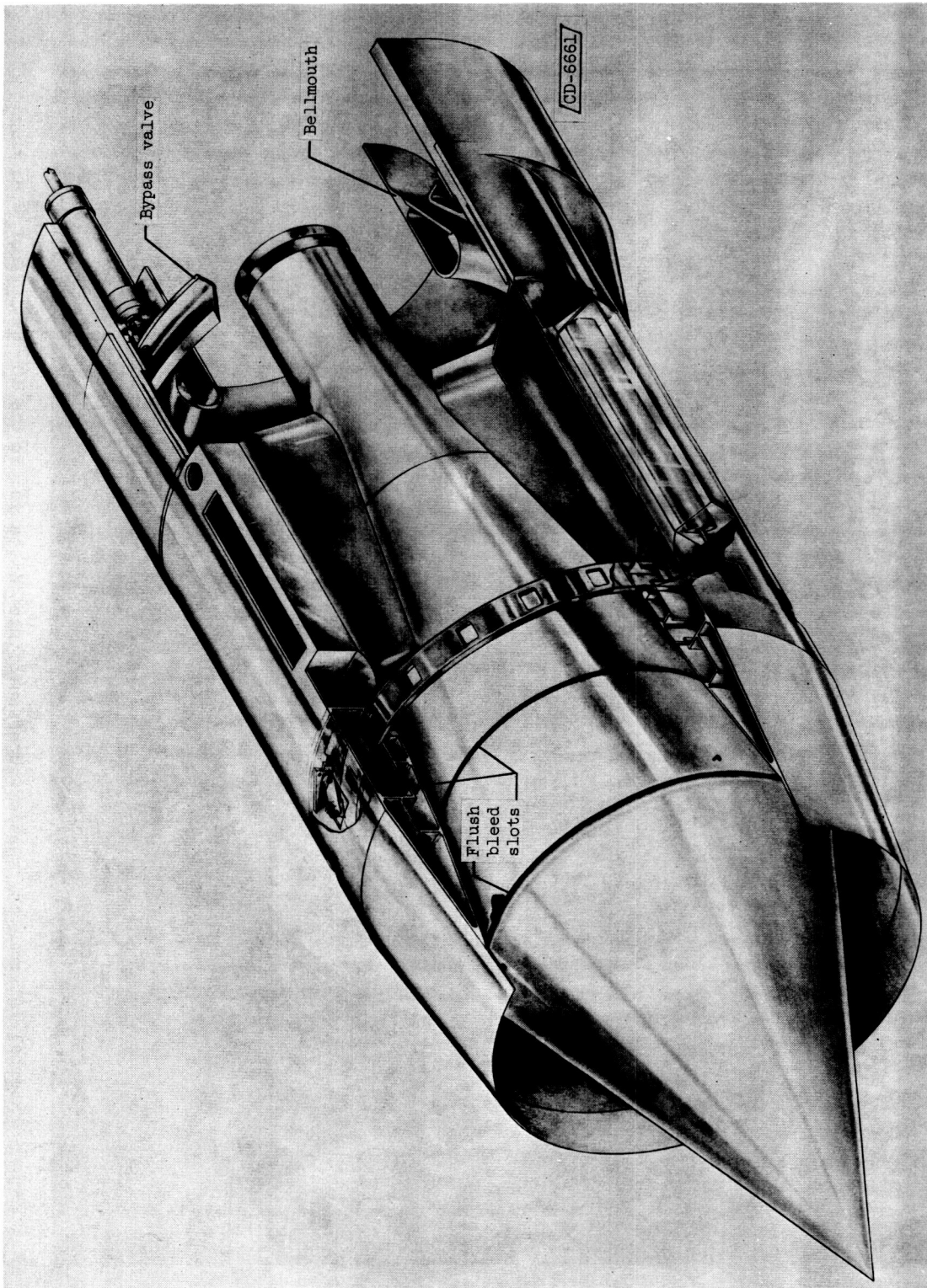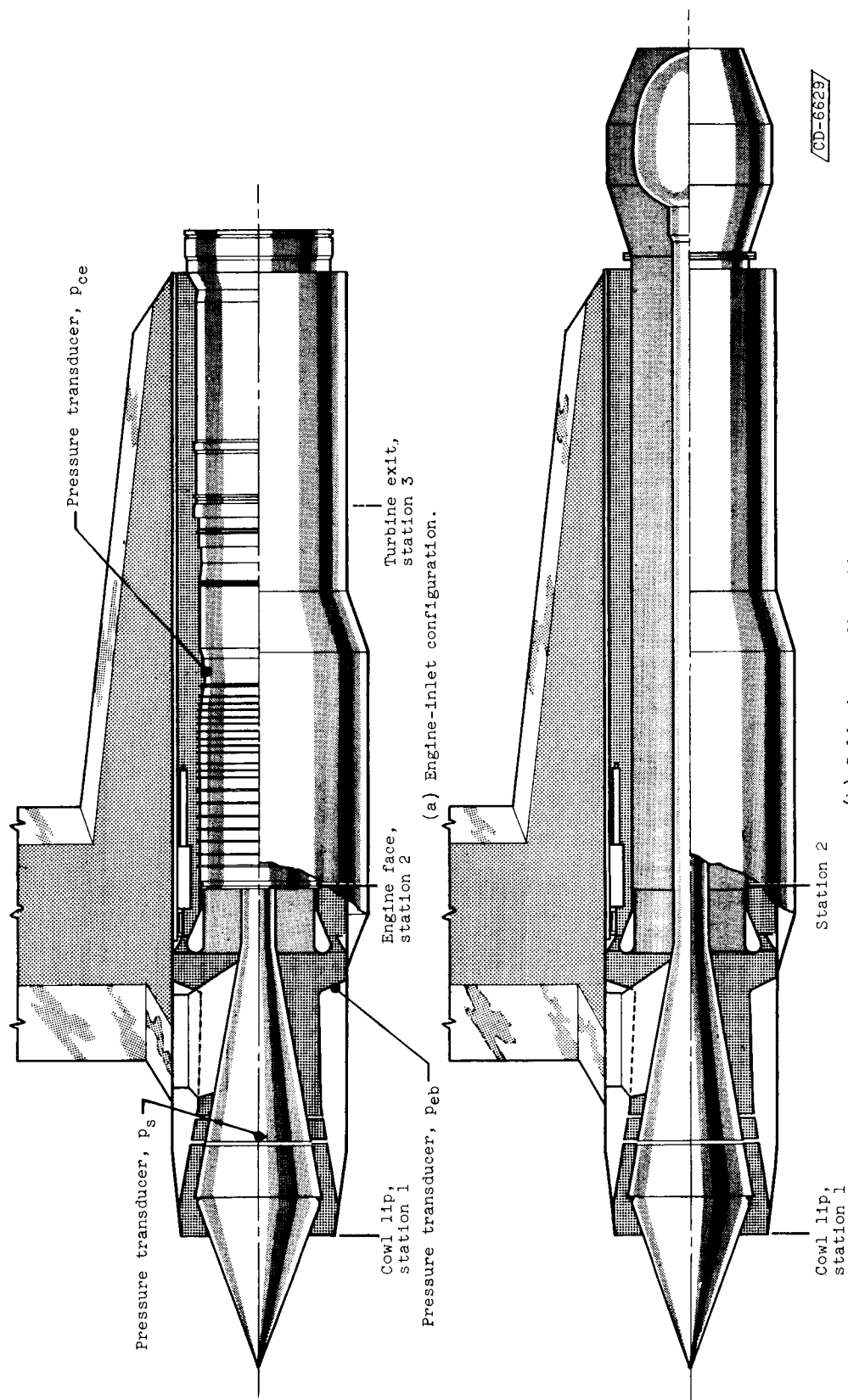Figure 1. - External-internal-compression supersonic inlet installed in the 10- by 10-foot wind tunnel.

Figure 2. - Cutaway of inlet.

Bypass valve

Bellmouth

CD-6661

Flush bleed slots

E-649

Pressure transducer, p_{ce}

Turbine exit,
station 3

(a) Engine-inlet configuration.

Engine face,
station 2

Pressure transducer, p_s

Pressure transducer, p_{eb}

Cowl lip,
station 1

Station 2

(b) Cold-pipe configuration.

Cowl lip,
station 1

CD-6629

Figure 3. - Cutaway of nacelle showing installation of J79 and cold pipe.

16
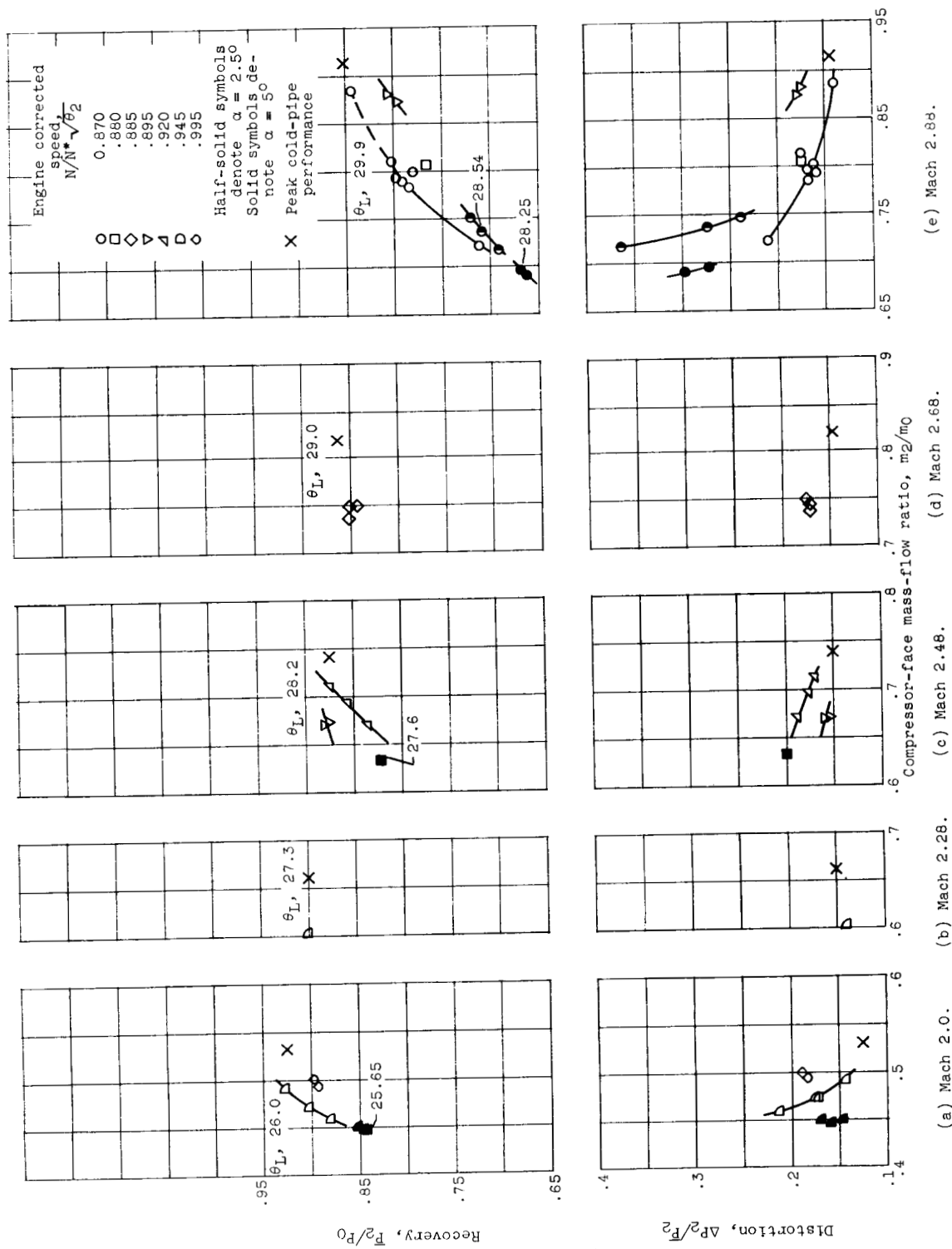
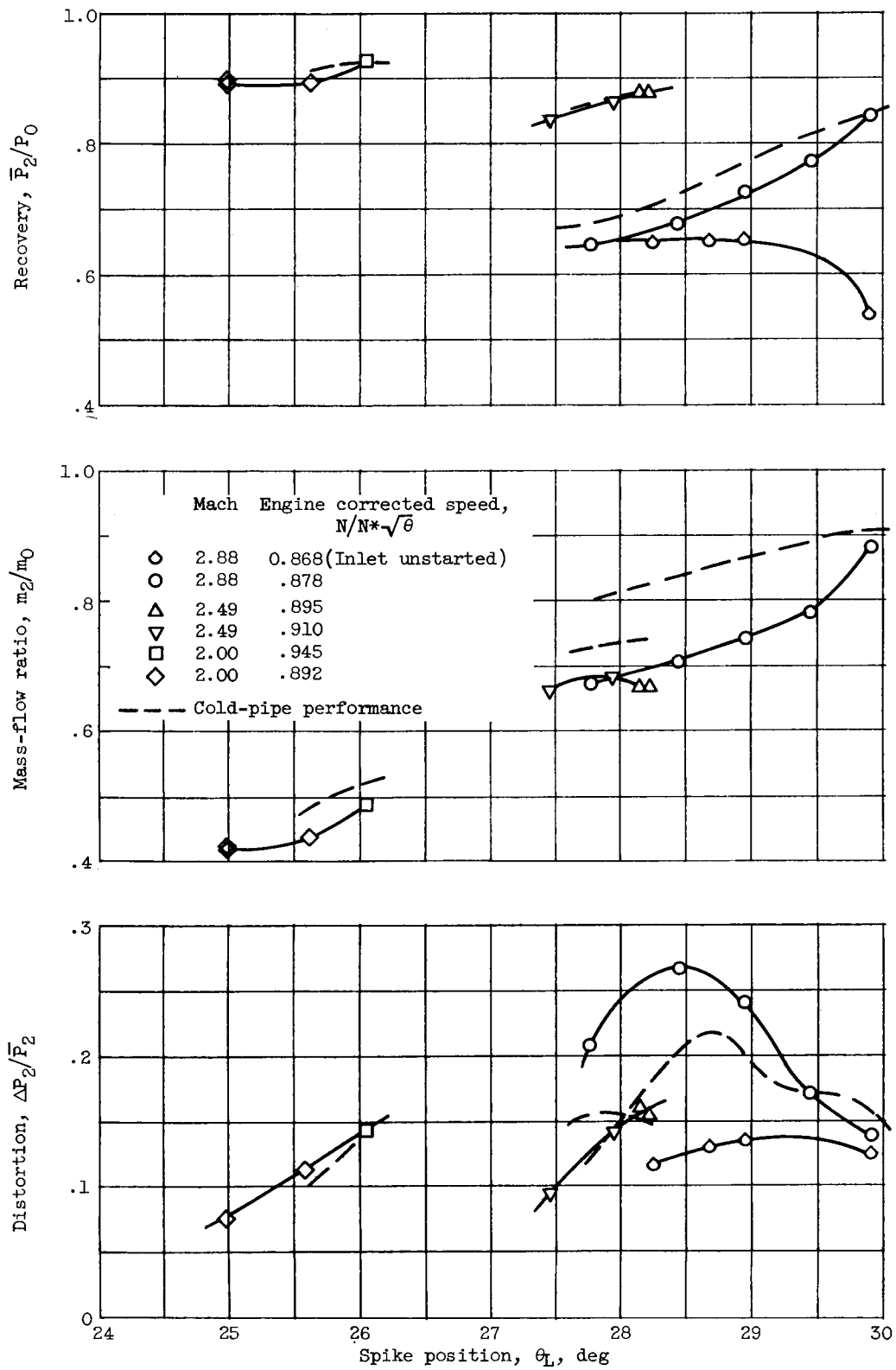Figure 4. - Engine-inlet performance at maximum contraction.

(a) Mach 2.0. (b) Mach 2.28. (c) Mach 2.48. (d) Mach 2.68. (e) Mach 2.88.

E-649

CT-3

Recovery, $\bar{P}_2/P_0$

Mass-flow ratio, m_2/m_0

	Mach	Engine corrected speed, $N/N*\sqrt{\theta}$
◇	2.88	0.868(Inlet unstarted)
○	2.88	.878
△	2.49	.895
▽	2.49	.910
□	2.00	.945
◇	2.00	.892
– – –	Cold-pipe performance	

Distortion, $\Delta P_2/\bar{P}_2$

Spike position, θ_L, deg

Figure 5. - Engine-inlet performance at less than maximum contraction.

18

$p_2/\overline{P}_O$, 0.771
$\Delta P_2/\overline{P}_2$, 0.142
$\overline{P}_2/P_O$, 0.844
θ_L, 29.96

(a) Peak recovery at Mach 2.88
and α = 0°.

$p_2/\overline{P}_O$, 0.603
$\Delta P_2/\overline{P}_2$, 0.254
$\overline{P}_2/P_O$, 0.668
θ_L, 28.29

(b) Peak recovery at Mach 2.88
and α = 5°.

$p_2/\overline{P}_O$, 0.634
$\Delta P_2/\overline{P}_2$, 0.219
$\overline{P}_2/P_O$, 0.728
θ_L, 28.72

(c) Peak recovery with spike extended
at Mach 2.88 and α = 0°.

$p_2/\overline{P}_O$, 0.688
$\Delta P_2/\overline{P}_2$, 0.200
$\overline{P}_2/P_O$, 0.789
θ_L, 30.04

(d) Below peak recovery at Mach 2.88
and α = 0°.

$p_2/\overline{P}_O$, 0.709
$\Delta P_2/\overline{P}_2$, 0.202
$\overline{P}_2/P_O$, 0.605
θ_L, 27.53

(e) Peak recovery at Mach 2.48
and α = 5°.

$p_2/\overline{P}_O$, 0.714
$\Delta P_2/\overline{P}_2$, 0.157
$\overline{P}_2/P_O$, 0.841
θ_L, 25.65

(f) Peak recovery at Mach 2.00
and α = 5°.

Figure 6. - Typical compressor-face profiles from cold-pipe data.

(a) Mach 2.88; α, 0°.

	$\overline{P}_2/P_0$	m_2/m_0
O Cold pipe	0.849	0.825
□ Engine	.843	.885

(b) Mach 2.88; α, 2.5°.

	P_2/P_0	m_2/m_0
	0.701	0.69
	.720	-----

(c) Mach 2.48; α, 0°.

Cold pipe	0.884	0.698
Engine	.879	.668

(d) Mach 2.48; α, 5°.

	0.805	0.589
	.823	.631

(e) Mach 2.00; α, 0°.

Cold pipe	0.930	0.487
Engine	.927	.491

(f) Mach 2.00; α, 5°.

	0.841	0.460
	.845	.457

P_2/P_0
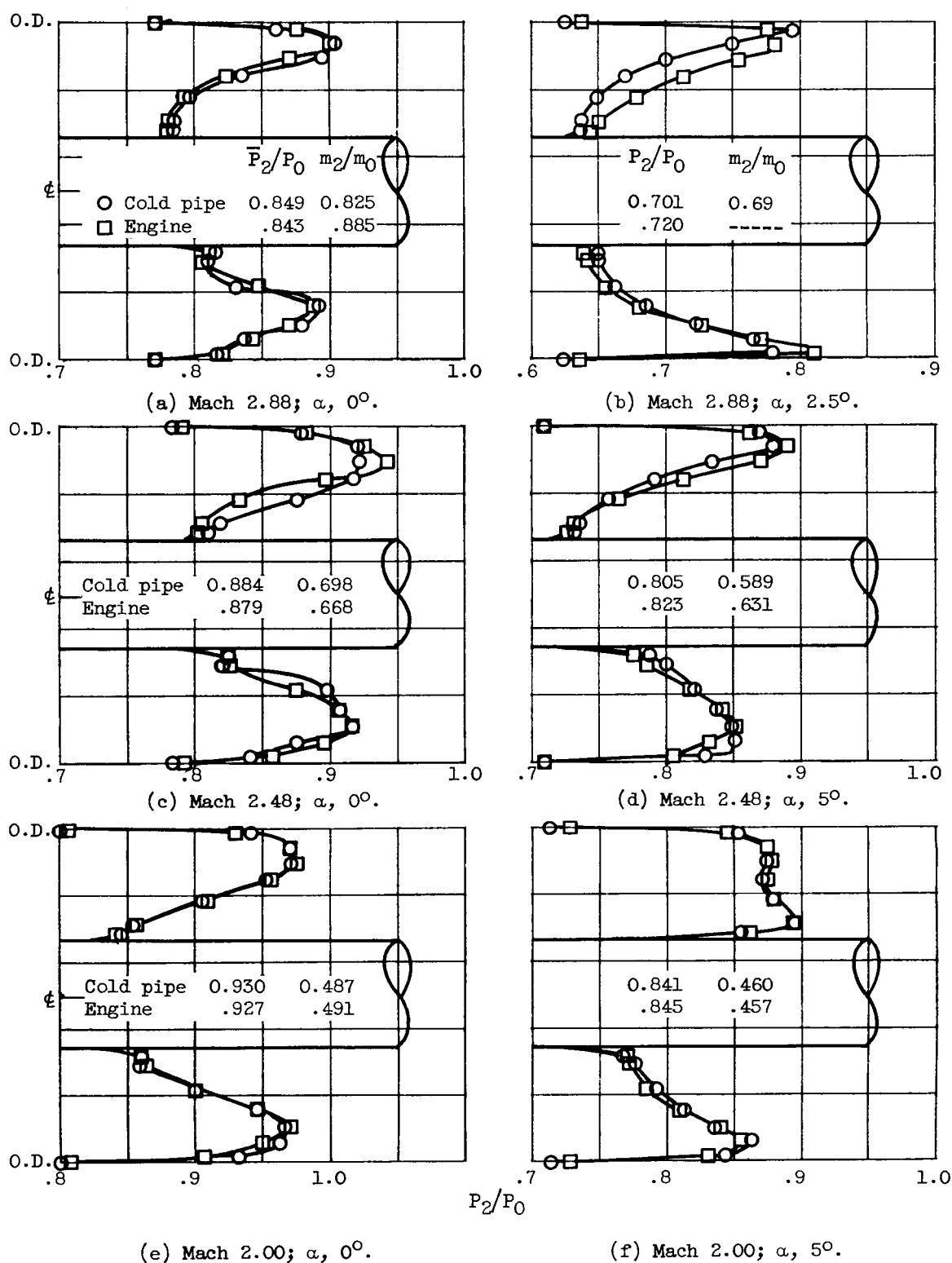
Figure 7. - Comparison of total-pressure profile from identical rakes in engine and cold-pipe configurations.
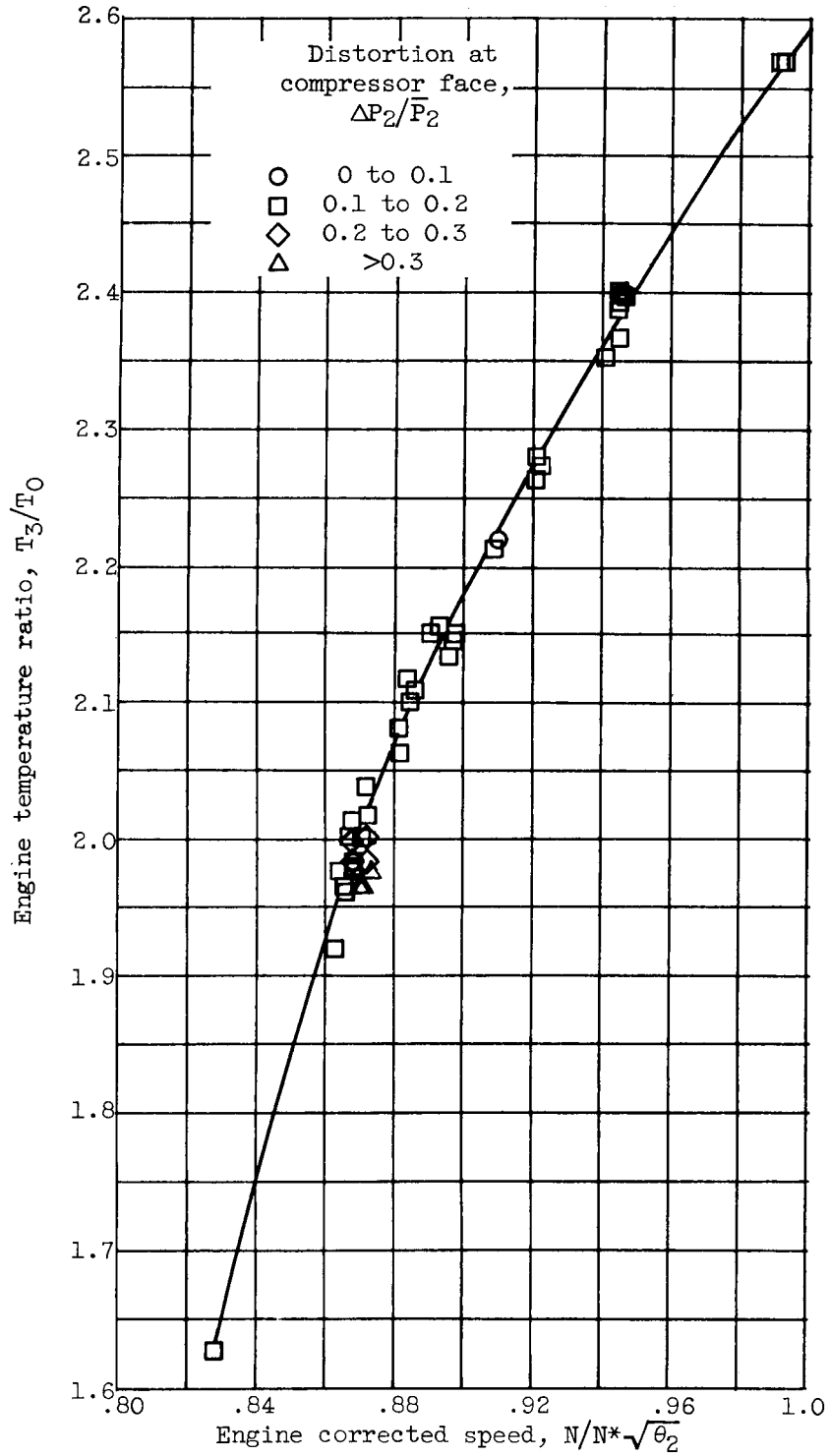
(a) Engine temperature ratio.

Figure 8. - Effect of distortion on engine performance.
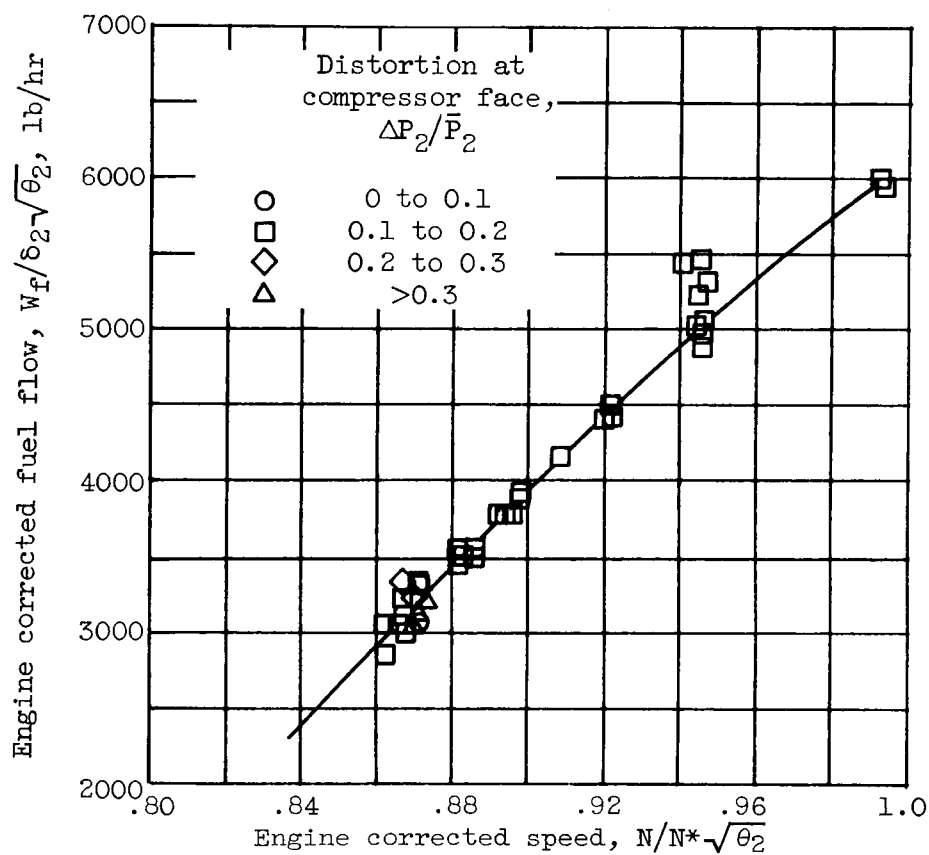
(b) Engine corrected fuel flow.

Figure 8. - Continued. Effect of distortion
on engine performance.
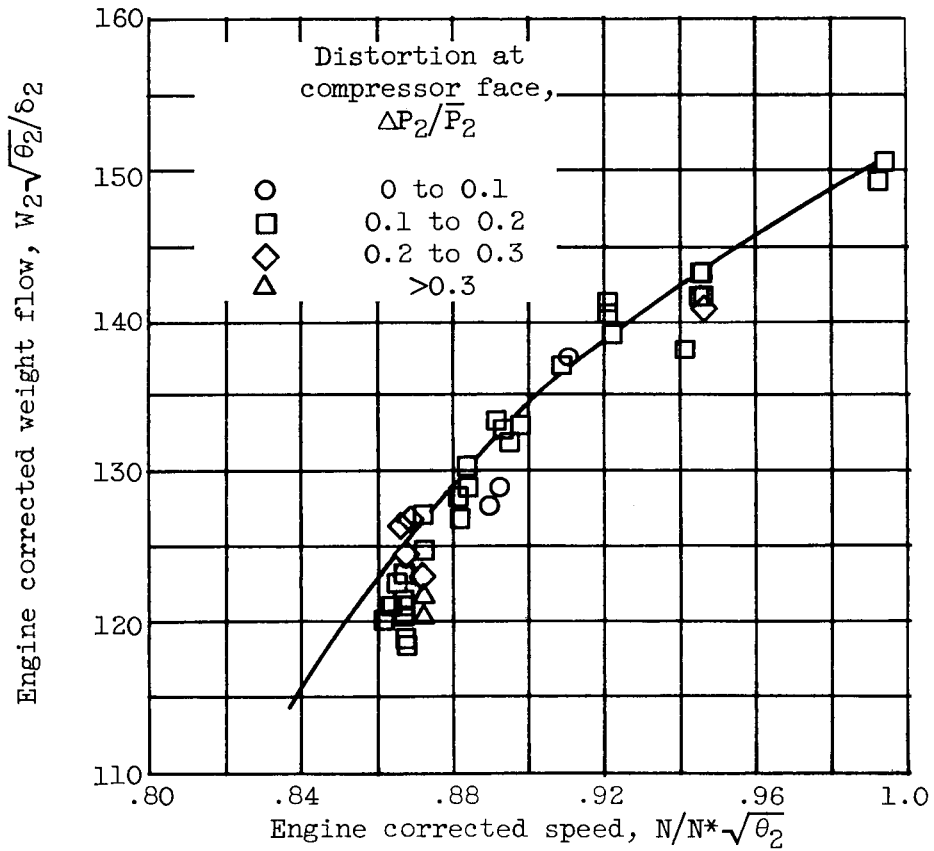
(c) Engine corrected weight flow.

Figure 8. - Continued. Effect of distortion on engine performance.
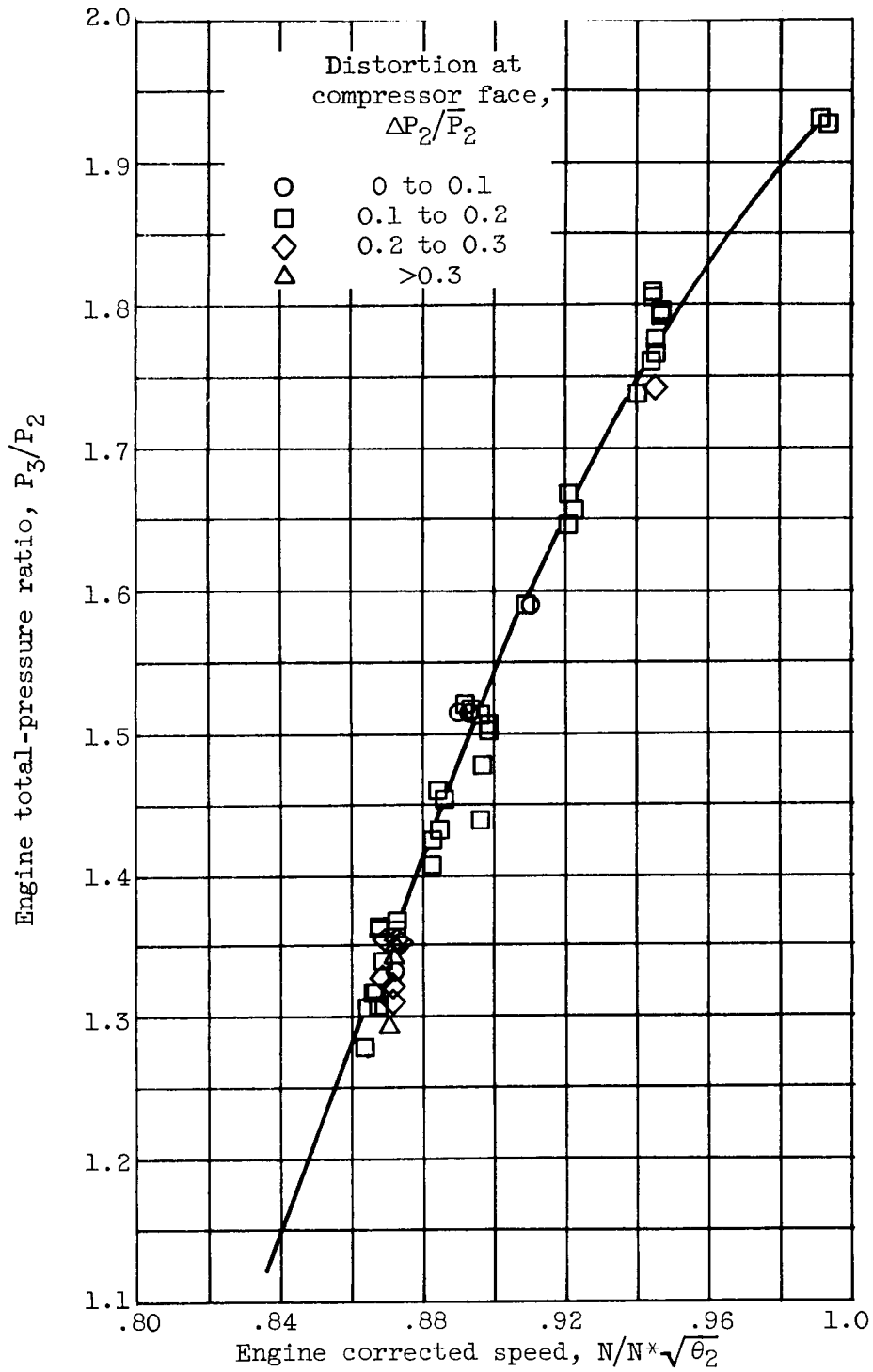
(d) Engine total-pressure ratio.

Figure 8. - Concluded. Effect of distortion on
engine performance.

E-649
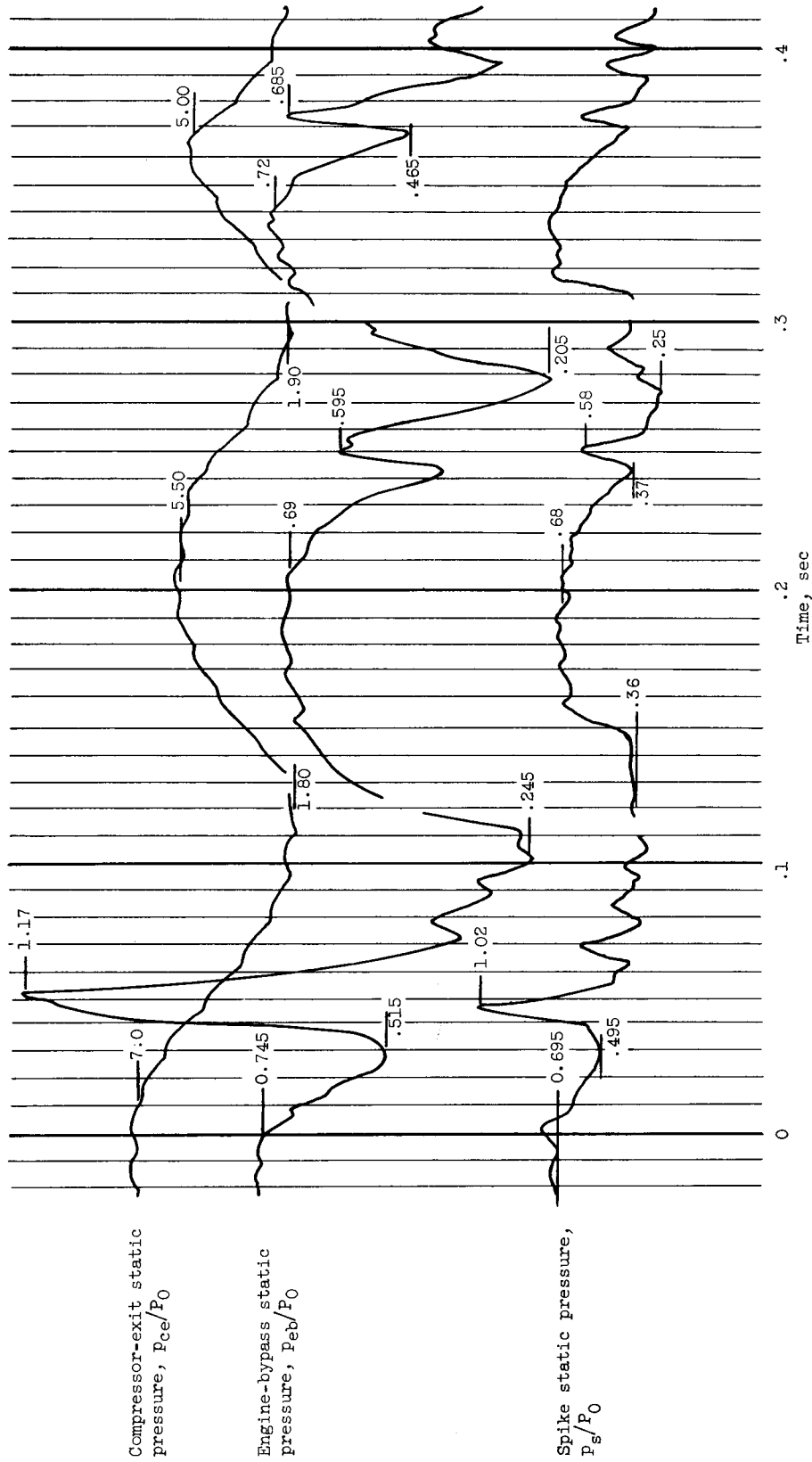
(a) Mach 2.48; α, 0°; $N/N*\sqrt{\theta}$, 0.896; θ_{IGV}, 3.5°; θ_L, 28.20.

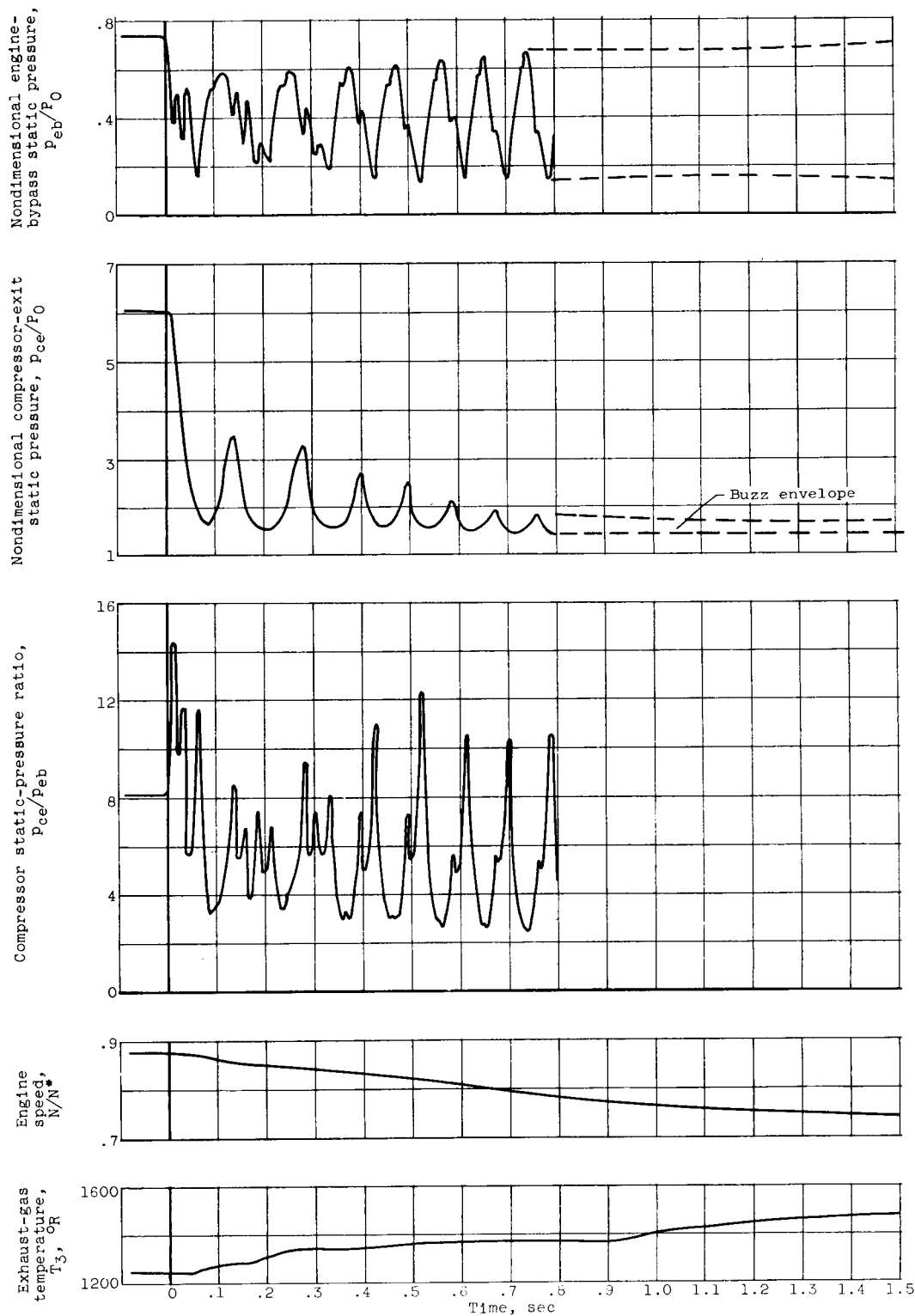Figure 9. - Trace of compressor-exit, engine-bypass, and spike static pressures during inlet unstarting.

Compressor-exit static
pressure, p_{ce}/P_0

Engine-bypass static
pressure, p_{eb}/P_0

Spike static pressure,
p_s/P_0

Time, sec
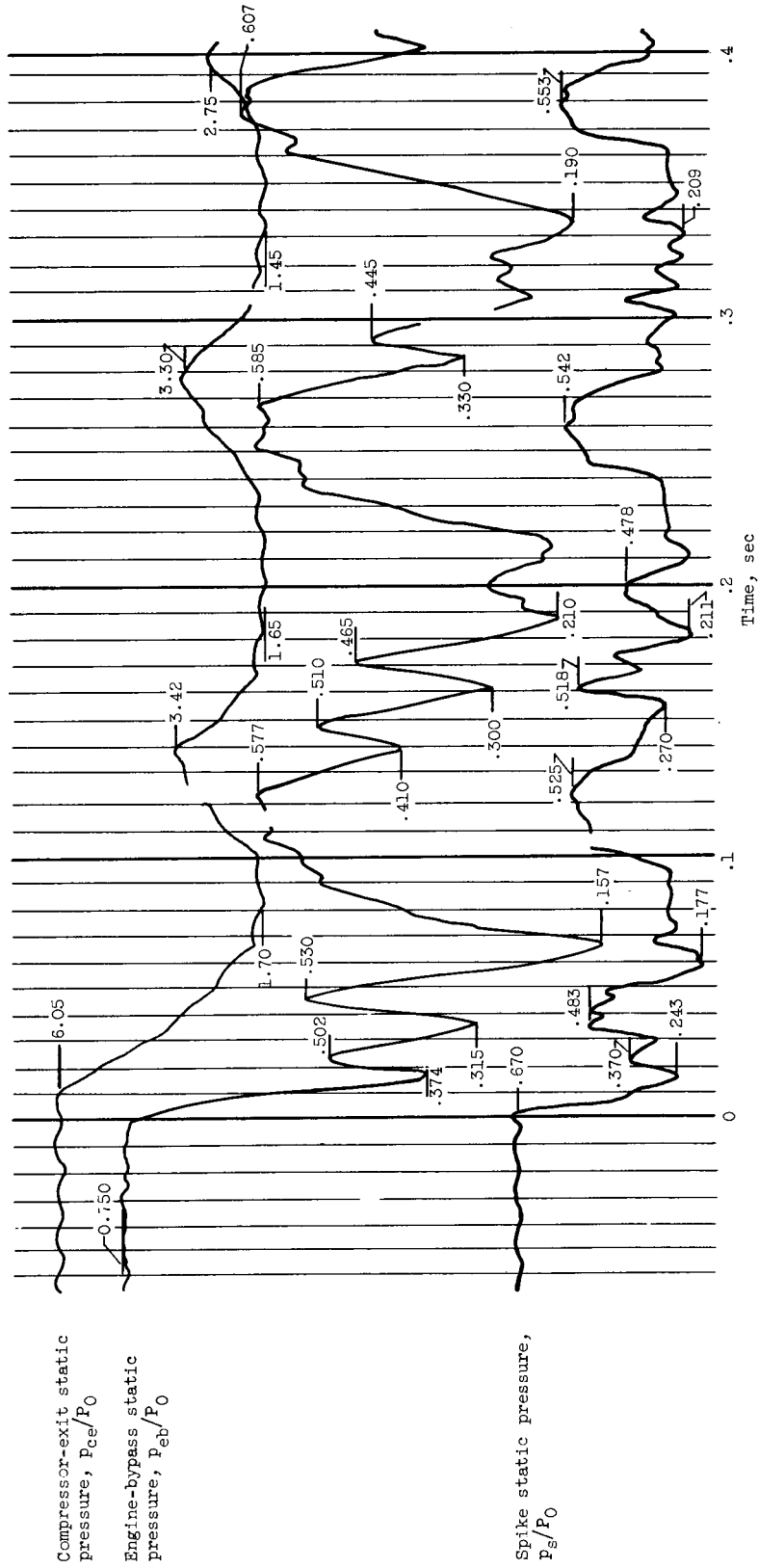
(b) Mach 2.88; α, 0°; $N/N^*\sqrt{\theta}$, 0.872; θ_{IGV}, 3.3°; θ_L = 29.90.

Figure 9. - Concluded. Trace of compressor-exit, engine-bypass, and spike static pressures during inlet unstarting.
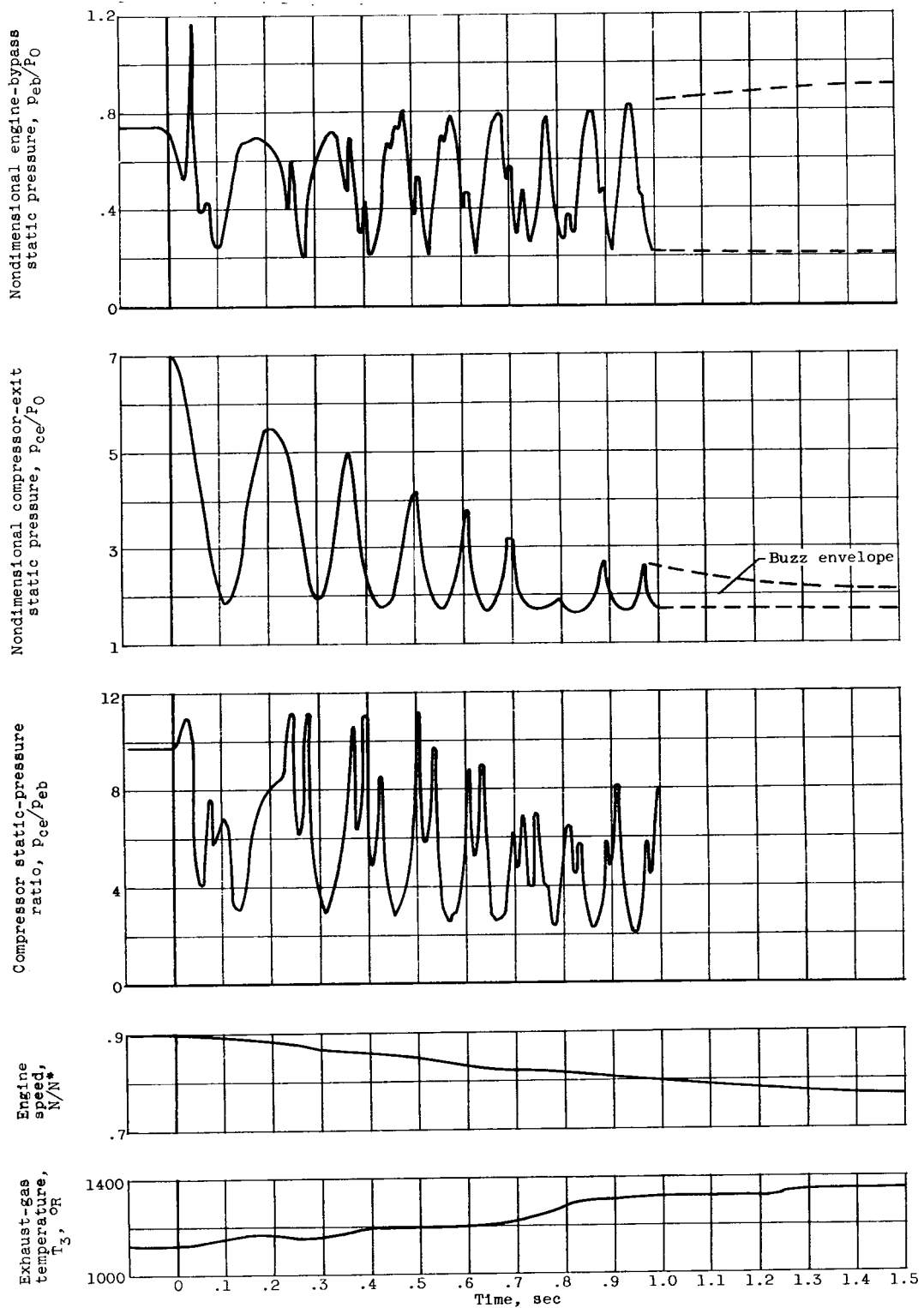
(a) Mach 2.48; α, 0°; θ_{IGV}, 3.5°.

Figure 10. - Inlet pressure variation and engine performance immediately after unstarting of inlet.
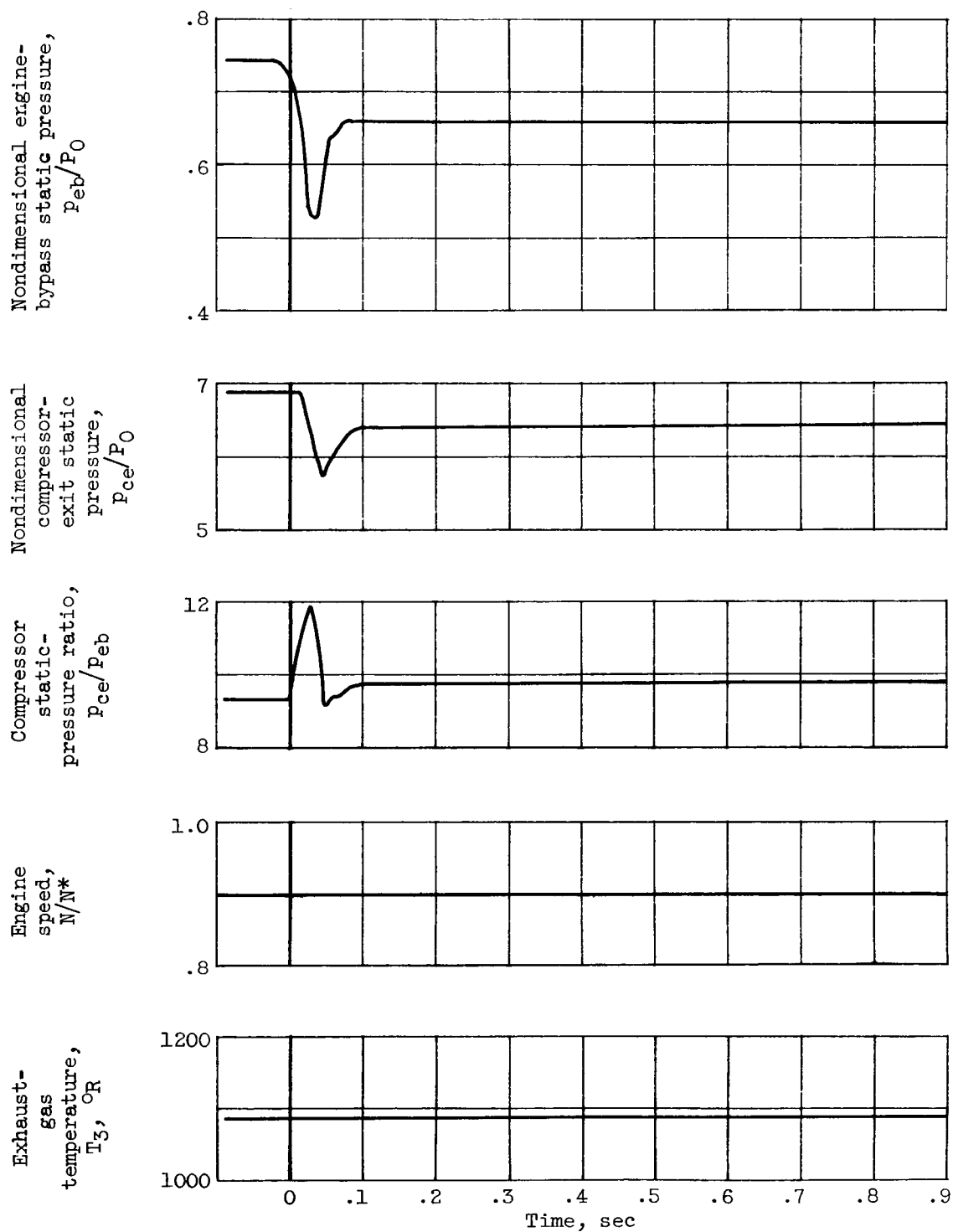
E-649

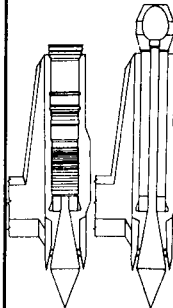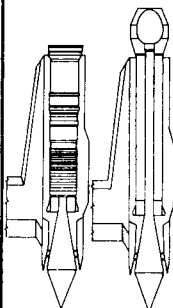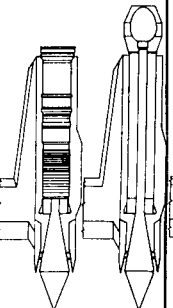(c) Mach 2.88; α, 0°; θ_{IGV}, 5.5^o.

Figure 10. - Concluded. Inlet pressure variation and engine performance immediately after unstarting of inlet.
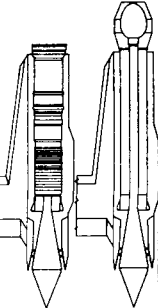
E-649

NOTES: (1) Reynolds number is based on the diameter of a circle with the same area as that of the capture area of the inlet.

(2) The symbol * denotes the occurrence of buzz.

INLET BIBLIOGRAPHY SHEET

Report and facility	Description			Test parameters					Test data			Performance		Remarks
	Configuration	Number of oblique shocks	Type of boundary-layer control	Free-stream Mach number	Reynolds number × 10⁻⁶	Angle of attack, deg	Angle of yaw, deg	Drag	Inlet-flow profile	Discharge-flow profile	Flow picture	Maximum total-pressure recovery	Mass-flow ratio	
CONFID. TM X-254 Lewis 10-by 10-ft supersonic wind tunnel		3	Flush slots	2.0 2.28 2.48 2.68 2.88	2.5	0°,5° 0° 0°,5° 0° 0°,2.5°,5°	0	No		Yes		0.927 .90 .875 .85 .843	0.49 .60 .71 .745 .885	Performance of both engine and inlet are presented. Also presented is the effect of unstarting the inlet on engine operation.
CONFID. TM X-254 Lewis 10-by 10-ft supersonic wind tunnel		3	Flush slots	2.0 2.28 2.48 2.68 2.88	2.5	0°,5° 0° 0°,5° 0° 0°,2.5°,5°	0	No		Yes		0.927 .90 .875 .85 .843	0.49 .60 .71 .745 .885	Performance of both engine and inlet are presented. Also presented is the effect of unstarting the inlet on engine operation.
CONFID. TM X-254 Lewis 10-by 10-ft supersonic wind tunnel		3	Flush slots	2.0 2.28 2.48 2.68 2.88	2.5	0°,5° 0° 0°,5° 0° 0°,2.5°,5°	0	No		Yes		0.927 .90 .875 .85 .843	0.49 .60 .71 .745 .885	Performance of both engine and inlet are presented. Also presented is the effect of unstarting the inlet on engine operation.
CONFID. TM X-254 Lewis 10-by 10-ft supersonic wind tunnel		3	Flush slots	2.0 2.28 2.48 2.68 2.88	2.5	0°,5° 0° 0°,5° 0° 0°,2.5°,5°	0	No		Yes		0.927 .90 .875 .85 .843	0.49 .60 .71 .745 .885	Performance of both engine and inlet are presented. Also presented is the effect of unstarting the inlet on engine operation.

Bibliography

These strips are provided for the convenience of the reader and can be removed from this report to compile a bibliography of NASA inlet reports. This page is being added only to inlet reports and is on a trial basis.